Materials Research Proceedings **25** (2023) 27-34 https://doi.org/10.21741/9781644902417-4

Numerical and experimental study of high-speed blanking of DC06 steel

E. Galiev[1a*], S. Winter[1b], M. Linnemann[1c], L. Winter[2d], V. Psyk[1e], V. Kräusel[1f]

[1] Fraunhofer Institute for Machine Tools and Forming Technology IWU, Reichenhainer Strasse 88, 09126 Chemnitz, Germany

[2] Institute of Materials Science and Engineering, Chemnitz University of Technology Erfenschlager Strasse 73, 09125 Chemnitz, Germany

[a*] elmar.galiev@iwu.fraunhofer.de, [b] sven.winter@iwu.fraunhofer.de, [c] maik.linnemann@iwu.fraunhofer.de, [d] lisa.winter@mb.tu-chemnitz.de, [e] verena.psyk@iwu.fraunhofer.de, [f] verena.kraeusel@iwu.fraunhofer.de

Keywords: Simulation, Blanking, High-Speed Impact Cutting

Abstract. In high-speed forming processes, such as electromagnetic forming or adiabatic blanking, the yield stress of the material is influenced by two opposing effects: deformation hardening and thermal softening due to adiabatic heating. In most cases, it is difficult to determine the temperature in the deformation zone in the process, due to closed tools. In this study, the tool for high-speed blanking was modified to access the measuring technique to enable recording the temperature in the deformation zone of a 3 mm thick DC06 steel with a high-speed pyrometer. The experimental results validated numerical calculations in LS-DYNA using the strain rate-dependent plastic model and the GISSMO material damage model. The reached temperatures in the shear zone ranged from 225 °C in case of a cutting punch velocity of 6.15 m/s) to 345 °C in case of a cutting punch velocity of 9.64 m/s. Thus, the study shows that the used numerical model and the damage model have a great potential for the simulation of high-speed blanking processes.

Introduction

In the sheet metal processing industry, cutting processes play an important role due to their high cost-effectiveness [1]. Almost every structural component is subject to at least one cutting process during its production [2]. Due to the increasing complexity of part geometries and the use of high-strength materials [3] often traditional blanking techniques, are not able to cope with the quality requirements imposed for the resulting cut surface [4]. An alternative to conventional cutting by shearing is adiabatic blanking or high-speed impact cutting (HSIC) [5]. The adiabatic blanking process is performed using a cutting tool speed of more than 3 m/s and a local strain rate above 10^3 s^{-1} [6]. These parameters result in a local temperature increase in the shear zone during the process, since the heat resulting from the energy released cannot dissipate during the short process time. In general, the development and change of temperature in the fracture region of a material is extremely important [7] and can explain many phenomena occurring in the material, which are often misinterpreted as caused by the strain rate [8]. These two important effects, temperature dependence and strain rate dependence of a materials plasticity, damage and failure behavior, are fundamental for creating a material model that approximates the real process. In the high strain rate regime, experimental process analysis and process design are much more complicated, since the measuring equipment is limited with respect to measurement frequency, and the area where the local temperature maximum is reached shortly before material failure is relatively small. In addition, most high-speed forming processes are performed in closed working tools without the possibility of access to measuring equipment.

It is well known that having a high-quality FEM model is key to cost-effective industrial implementation of production processes. Modern process simulation requires constitutive material

models to describe plasticity. These models must reflect the essential relationships between yield strength and stress state, strain, strain rate and temperature for the specific material [9]. In the particular case of high-speed blanking, strain rates in the range of 10^3 s^{-1} and higher require a wide range of yield curves and a suitable material damage model enabling the simulation of locally extremely high temperature changes in the fracture region. Here, the temperature in the shear zone is one of the dominant factors influencing the failure and further the quality of the cut surface. Thus, in the present study, for the first time, the temperature during HSIC will be measured directly in the shear zone using a specially modified tool and matched to a numerical model. The process validation will thus lead to a higher process understanding.

Materials and Methods

For the experimental HSIC tests and the subsequent numerical validation of the temperature, the steel DC06 was selected in a sheet metal thickness of 3 mm. The chemical composition of the used material received from the material supplier is shown in Tab. 1.

Tab. 1. Chemical compositions of the investigated steel DC06

	Composition (in wt-%)							
DC06	C	Si	Mn	S	Al	Ti	Nb	Fe
	0.007	0.01	0.12	0.00	0.06	0.06	0.01	bal.

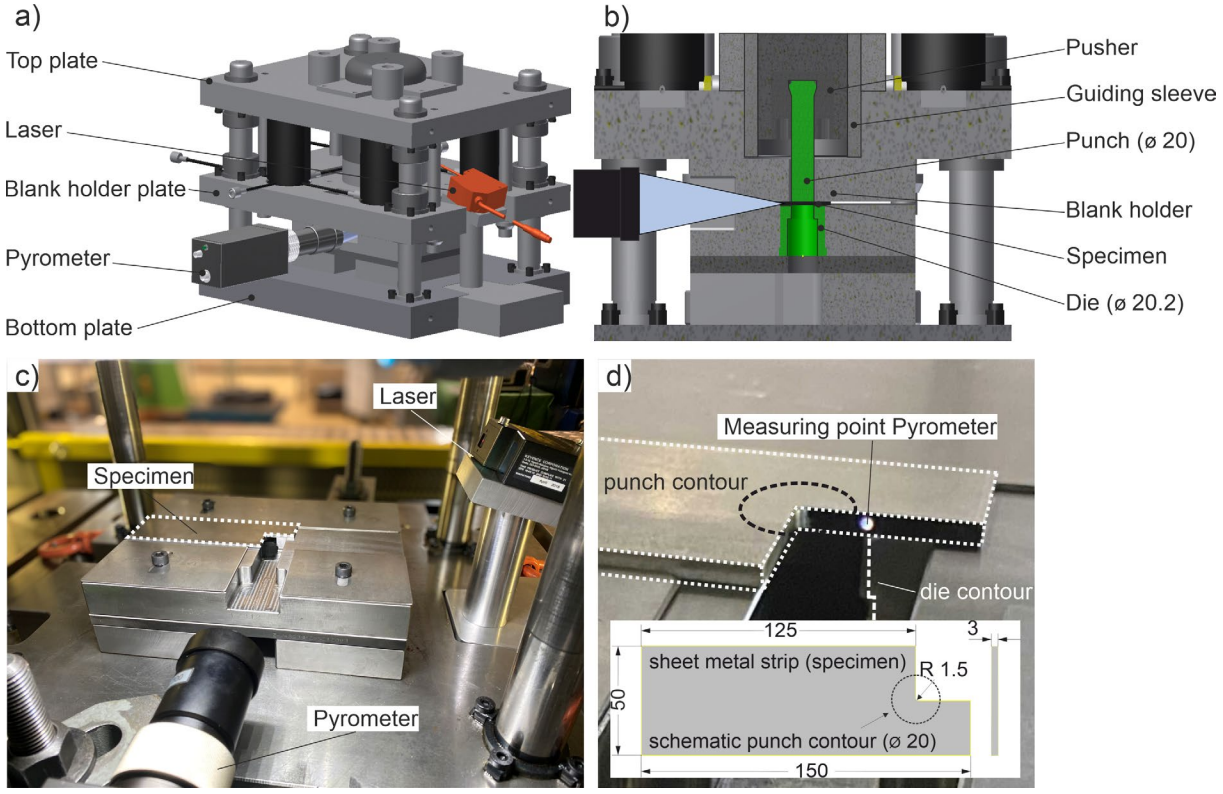

Fig. 1: Experimental setup for the HSIC tests. a) and b) CAD drawing of the tool with positioning of the measuring equipment and the relevant components. c) and d) Specimen geometry and position of the measuring point of the pyrometer.

The experimental tests were carried out on a high-speed ADIAflex press by MPM (Saint-Etienne, France). The tool shown in Fig. 1a was used for the cutting tests. The punch used had a diameter of 20 mm and the die had a diameter of 20.2 mm resulting in a mean circumferential cutting gap of 0.1 mm. For the used sheet thickness of 3 mm this cutting gap corresponds to a relative clearance of 3.33 %. Tests were performed at an energy level of 250, 500, 750, and 1000 J

(adjustable machine parameter). The corresponding punch speed and the resulting temperature in the shear zone were determined using a tool-integrated LKH-157 laser displacement measurement system from Keyence (Neu-Isenburg, Germany) and an IGA 740 high-speed pyrometer from LumaSense Technologies GmbH (Raunheim, Germany). The pyrometer has a working range of 160 °C - 1000 °C and an extremely high sampling rate of 166 kHz. To allow for a temperature measurement directly in the cutting zone (Fig. 1b), the sheets under investigation were pre-cut before the experiments (Fig. 1c and d). Precisely, a square with 25 mm side length was cut out at the outer edge. Consequently, the pyrometer could obtain the temperature directly in the center of the shear zone during the cutting test. The measuring area has a diameter of 0.7 mm (Fig. 1d) and the output data of the pyrometer is an integral quantity representative for the entire measurement area. The punch velocity was used as input parameter for the numerical simulation and the temperature measurement was used to validate the numerical model. In addition, the cut surfaces were evaluated with regard to the rollover height, the burnish and the fracture surface.

FE-Simulation

FE Analysis was performed using the explicit thermal and mechanical solver in the commercial software from LS-DYNA (DYNAmore GmbH, Stuttgart, Germany). The plastic deformation behavior of the material was described using the classical *MAT 024 PIECEWISE LINEAR PLASTICITY model [10], using different strain rate dependent yield curves. Details of this model including the yield curves used are described in [11]. Strain rate dependant damage and failure was modeled via the GISSMO damage and failure model developed by Neukamm et al. [12]. This model combines the damage description, which is used to calculate crash simulations, and an incremental formulation for the description of the material instability and localization. This fracture model can be used as a complement to the plastic material model and is specified using the *MAT_ADD_EROSION file. More detailed parameters for this fracture model are presented in [13].

Due to the geometry of the precut sheet, the stress distribution in the shear zone is inhomogeneous. Therefore, it was necessary to simulate the full geometry of the setup without exploiting any simplifications due to symmetry. The simulations of the high-speed blanking of the precut sheet metal specimens were performed with fully integrated solid elements (ELFORM 1) with edge lengths of 0.1x0.1x0.1 mm for test specimen and LS-DYNA R12.0.0. Fig. 2 shows the model consisting of a punch, a blank holder, a die, and a specimen. All parts of the model except the direct sample were specified as rigid bodies. The blankholder force was set to 80 kN and the friction coefficient was set to 0.15. The punch speed obtained from the experiment was specified as input information for the simulation using the *BOUNDARY_PRESCRIBED_MOTION file.

The temperature distribution was calculated via the dissipated forming energy according to Eq. 1 based on the temperature increase $\Delta\vartheta$, the specific heat capacity c_ϑ, the Taylor-Quinney factor κ [14], mass density ρ and the forming work performed ΔW_{dis}. The Taylor-Quinney factor is used to define the fraction of plastic stress power that is not converted into heat [15]. For the thermomechanical calculations performed in LS-DYNA $\kappa = 0.9$ was set.

$$\Delta\vartheta = \frac{\kappa \cdot \Delta W_{\mathrm{dis}}}{c_\vartheta \cdot \rho} \tag{1}$$

Materials Research Proceedings **25** (2023) 27-34 https://doi.org/10.21741/9781644902417-4

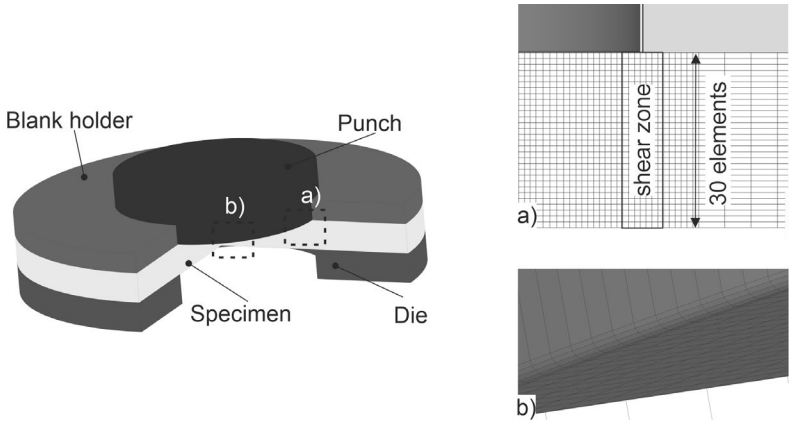

Fig. 2: Numerical model of the investigated HSIC process. a) Shear zone of the sheet metal specimen for the temperature calculation with fine mesh size. b) Punch with significantly larger mesh.

Results and Discussion

Fig. 3 summerizes results of the experimental determination of the punch velocity. The exemplary diagram shows three measured time-dependent displacement of the cutting punch as recorded by the laser displacement measurement system during tests at an energy level of 250 J together with the resulting mean value curve. The shape of the curve is representative for all measurements. The gradient of the curve in the region between Point 1 and Point 2 corresponds to the velocity during cutting. Subsequently, due to the impact, wave propagation occurs throughout the die and the punch consequently continues to move in a wave-like manner after the part is ejected, as documented by the curve after the straight initial line. For transfer to the numerical simulation, the gradient between Point 1 and 2 of the respective mean value curve was evaluated and transferred to the simulation as input variable for the punch velocity. The measured velocities for each energy level investigated here are shown in the table next to the curve (Fig. 3). The lowest energy reached a velocity of 6.15 m/s and the velocity increases with increasing energy as expected. At 1000 J the velocity was about 9.64 m/s.

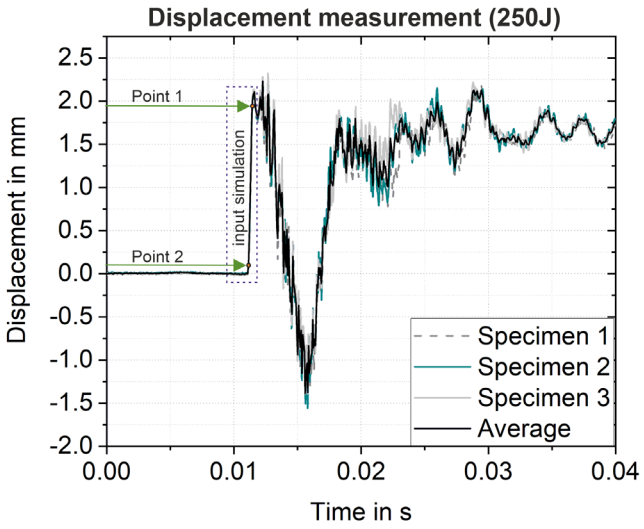

$$V_{Punch} = \frac{S_1 - S_2}{t_1 - t_2} = 6.147\ m/s$$

Energie	Velocity
250 J	6.147 m/s
500 J	8.244 m/s
750 J	8.978 m/s
1000 J	9.641 m/s

Fig. 3: Representative displacement-time measurements at an energy level of 250 J. The gradient of the curve between point 1 and 2 corresponds to the velocity and were used as input parameter for the numerical simulation. The measured velocities from 250 J to 1000 J are recorded in the table.

Materials Research Proceedings **25** (2023) 27-34 https://doi.org/10.21741/9781644902417-4

The HSIC tests at all four different energy levels led to complete separation of the parts in all cases (see Fig. 4). The optical microscopy images for the evaluation of the cut surface quality were all taken at maximum distance from the pre-cut area (Fig. 4, red marking). Regardless of the energy and the corresponding punch velocity, all specimens show excellent cut surfaces with very good quality. The parts have no burr and a rollover height of only 0.237–0.325 mm. The burnish is between 1.19–1.32 mm and the fracture surface between 1.41–1.51 mm. Significant differences or tendencies cannot be recognized, proving that even the lowest cutting speed or impact energy provides sufficient energy to cut the relatively soft steel DC06 (approx. 93 HV1) and to provide very good cut surface quality (no burr, very straight, high percentage of burnish).

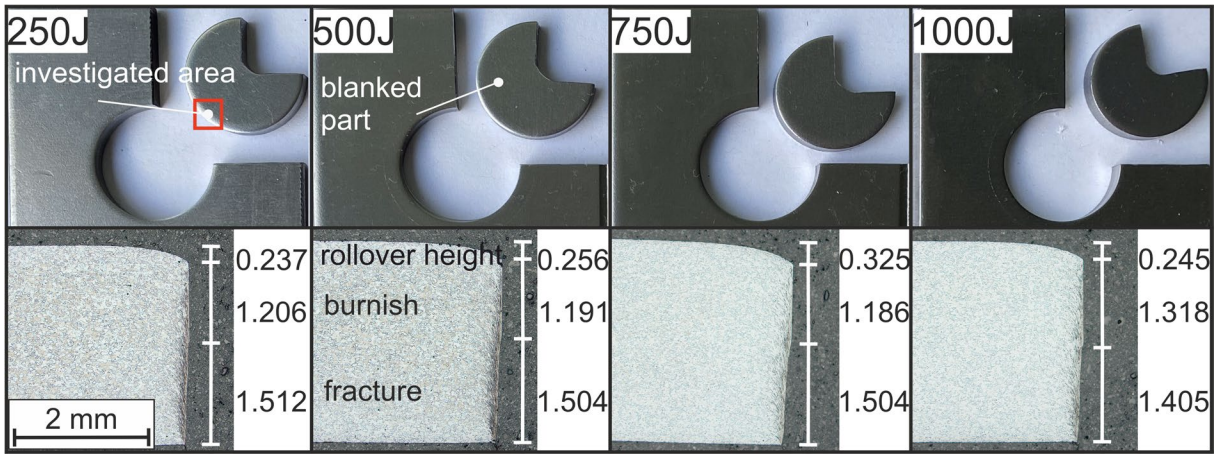

Fig. 4: Cut parts optical images of the corresponding cut surfaces produced using energy levels from 250 J to 1000 J. The rollover height, burnish and fracture surface fractions were measured in mm.

Fig. 5 shows the simulation results of the cutting process. Precisely, the temperature distribution in the circumferential shear zone at a penetration depth of the punch of 10 % of the sheet thickness is illustrated. The deformation and especially the temperature distribution shown here is highly inhomogeneous. In the area of the free surface where the temperature was measured in the experiment, the temperature maximum is 142 °C (see Fig. 5a). In the area of the longest distance to the measuring point, however, the temperature already reaches 242 °C (Fig. 5b). This can be explained by the free surface: Only on one side of this surface material can generate heat by deformation, while at the other side the material is cut away. In the experiment additional cooling effects due to convection can occur, but presumably these play a minor role and were therefore not considered in the simulation. Likewise, the slug is not moved homogeneously through the sheet, but is subject to bending stress. This proves that in order to simulate the process correctly, it is absolutely necessary to model the complete slug. Considering any symmetry in order to reduce calculation time will cause significant differences between experiment and simulation due to the inhomogeneous temperature distribution.

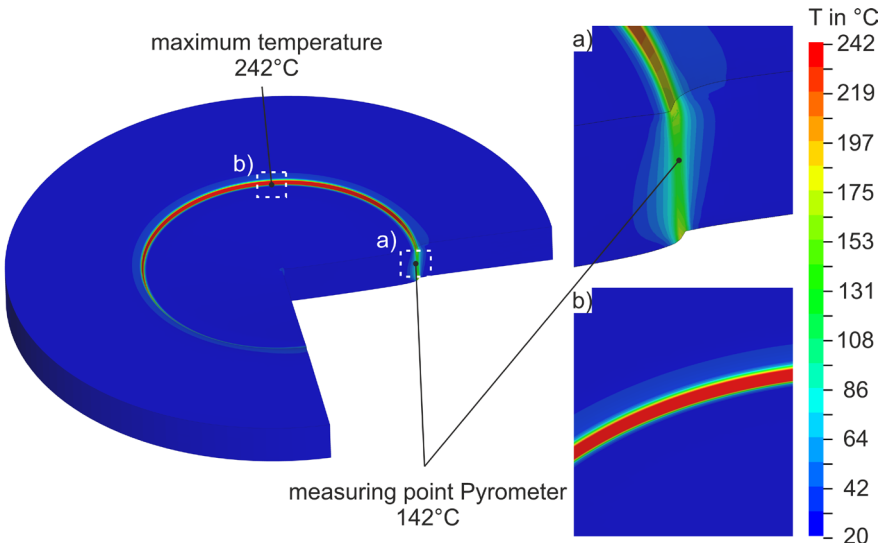

Fig. 5: Simulation of the pre-cut part at 9.64 m/s impact velocity with strongly inhomogeneous temperature distribution in the circumferential shear zone.

Fig. 6 shows an example of the numerically determined temperature distribution in the 2D section as a function of the punch penetration depth in the shear zone in the area of the measuring field of the pyrometer (cf. Fig. 5a) for a cutting operation with 9.641 m/s impact velocity (1000 J). The penetration depth is specified in relation to the sheet thickness. The qualitative temperature profile in the cutting test is identical for all investigated velocities. However, the maxima differ significantly (see Fig. 7). The maximum temperatures occur close to the contact surfaces between punch/sheet and sheet/die. The heat then propagates into the center of the shear zone. Due to the high velocity, the temperature increases only very locally and hardly spreads into the base material, so that the process can be considered quasi-adiabatic. The strong localization of heat leads to localized material softening, which counteracts the hardening during forming and can cause the formation of adiabatic shear bands in the shear zone [6]. The geometric properties (rollover height, burnish, fracture) of the cut surface formed at 25 % penetration depth are comparable to those of the real cut surface shown in Fig. 4. This demonstrates that the implemented damage model works well, even if it is only a qualitative comparison. The maximum temperature reached in Fig. 6 (at a penetration depth of 25 %) of 322 °C is not the maximum in the cutting process. This was reached just before failure and is discussed in Fig. 7.

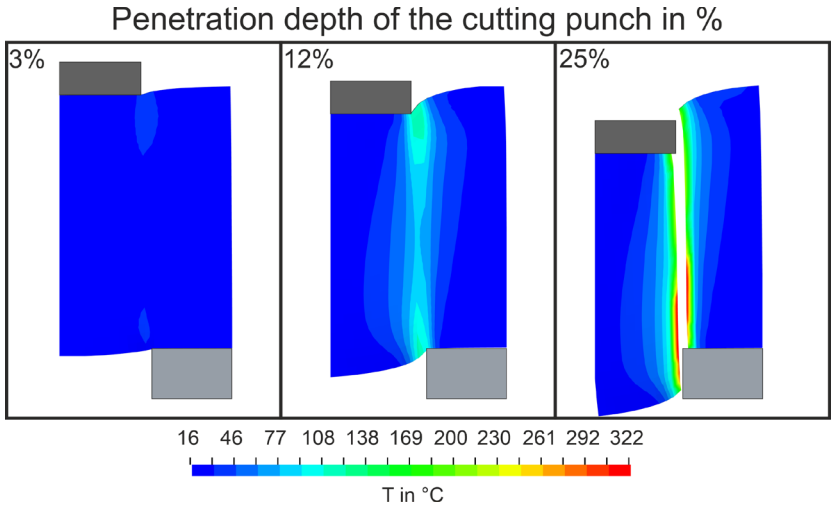

Fig. 6: Numerically determined temperature distribution in the 2D section as a function of the punch penetration depth for an impact velocity of 9.64 m/s.

The averaged results (3 samples for each velocity) of the temperature measurement by pyrometer and the numerically determined maximum temperatures are summarized in Fig. 7. For all velocity ranges from about 6.15 m/s to 9.64 m/s experimentally and numerically determined temperatures are in good agreement with each other. The temperatures in the experiment were between approx. 225 °C and 345 °C. In the simulation, the temperatures ranged between approx. 240 °C and 338 °C. Thus, the resulting standard deviation is 4.8% at 6.15 m/s, 5.4 % at 8.24 m/s, 1.7 % at 8.98 m/s, and 2.0 % at 9.64 m/s. The experimental data show that the temperature increases almost linearly with increasing velocity and consequently increasing energy.

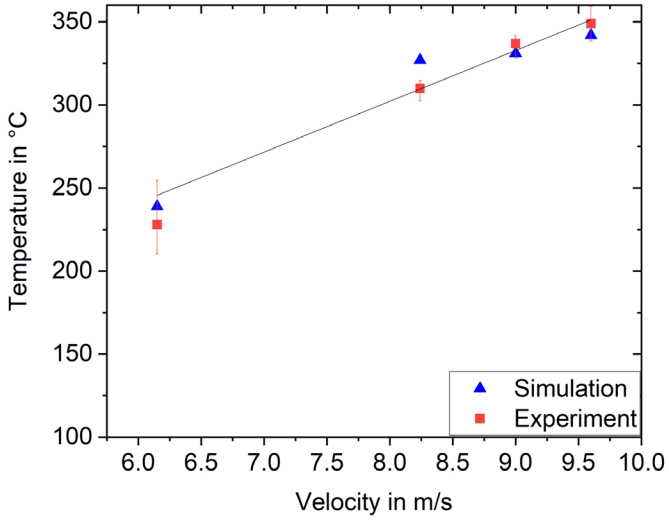

Fig. 7: Comparison of experimentally and numerically determined maximum temperatures in the shear zone at HSIC with four different punch velocities. The results are in very good agreement.

Summary and Conclusion

In the present work, a comprehensive numerical model was validated against a real HSIC process. Since the temperature in the shear zone plays a dominant role at high process speeds, validation was realized for the first time using a temperature in the shear zone measured by a high-speed pyrometer during HSIC. Numerically and experimentally, the good cold-formable steel DC06 was used. Extensive preliminary work [11]and the experimental velocity measurement from HSIC served as input for the material and GISSMO damage model used. It was necessary to model the cutting process completely, due to the non-rotationally symmetrical geometry of the part. Such geometries cause inhomogeneous temperature distributions in the shear zone. The extensive simulation made it possible to match the numerically determined temperature with the measuring field of the pyrometer. The results of numerical and experimental temperature determination showed almost identical temperatures (in the range of 225 to 345 °C) at four different test velocities (6.15 to 9.64 m/s). So the experimentally and numerically determined temperatures are in good agreement (standard deviation between 1.7 % and 5.4 %). It can be concluded that the extensive numerical model used is very well suited to represent the HSIC for the DC06 steel. The consideration of the local temperature in the shear zone enables a significantly higher accuracy. Therefore, the present results will significantly improve the numerical process design of the HSIC in future work.

References

[1] S.F. Golovashchenko, N. Wang, Q. Le, Trimming and sheared edge stretchability of automotive 6xxx aluminum alloys, J. Mater. Process. Technol. 264 (2019), pp. 64–75. https://doi.org/10.1016/j.jmatprotec.2018.09.001

[2] M.-L. Li, D.-S. Bi, J.-K. Hao, Automotive sheet metal SAPH440 and Q235 formability of comparative study, 2015 International Conference on Material Science and Applications (icmsa-15) : Atlantis Press, pp. 1027–1030

[3] K. Sugimoto, T. Hojo, A.K. Srivastava, Low and medium carbon advanced high-strength forging steels for automotive applications. Metals 9 (2019), Nr. 12, pp. 1263. https://doi.org/10.3390/met9121263

[4] A.K. Perka, M. John, U.B. Kuruveri, P.L. Menezes, Advanced High-Strength Steels for Automotive Applications: Arc and Laser Welding Process, Properties, and Challenges, In: Metals 12 (2022), Nr. 6, pp. 1051. https://doi.org/10.3390/met12061051

[5] S. Winter, M. Nestler, E. Galiev, F. Hartmann, V. Psyk, V. Kräusel, M. Dix, Adiabatic Blanking: Influence of Clearance, Impact Energy, and Velocity on the Blanked Surface, J. Manuf. Mater. Process. 5 (2021), Nr. 2, pp. 35. https://doi.org/10.3390/jmmp5020035

[6] F. Schmitz, S. Winter, T. Clausmeyer, M.F.-X. Wagner, A. E. Tekkaya, Adiabatic blanking of advanced high-strength steels, CIRP Ann. 69 (2020), Nr. 1, pp. 269–272. https://doi.org/10.1016/j.cirp.2020.03.007

[7] D.M. Neto, J.R. Barros, M.C. Oliveira, P.V. Antunes, A. Ramalho, R.L. Amaral, A.D. Santos, J.L. Alves, L.F. Menezes, Heat generation when forming AHSS: experimental and numerical analysis of tensile and draw-bead tests. IOP Conference Series: Materials Science and Engineering 967 (2020), Nr. 1, pp. 12086. https://doi.org/10.1088/1757-899X/967/1/012086

[8] P. Knysh, Y. P. Korkolis, Determination of the fraction of plastic work converted into heat in metals, Mech. Mater. 86 (2015), Nr. 3, pp. 71–80. https://doi.org/10.1016/j.mechmat.2015.03.006

[9] N. Abedrabbo, F. Pourboghrat, J. Carsley, John, Forming of AA5182-O and AA5754-O at elevated temperatures using coupled thermo-mechanical finite element models, Int. J. Plast. 23 (2007), Nr. 5, pp. 841–875. https://doi.org/10.1016/j.ijplas.2006.10.005

[10] F. Andrade, M. Feucht (Eds.): A comparison of damage and failure models for the failure prediction of dual-phase steels, 2017

[11] E. Galiev, S. Winter, F. Reuther, V. Psyk, M. Tulke, A. Brosius, V. Kräusel, Local Temperature Development in the Fracture Zone during Uniaxial Tensile Testing at High Strain Rate: Experimental and Numerical Investigations, Appl. Sci. 12 (2022), Nr. 5, pp. 2299. https://doi.org/10.3390/app12052299

[12] M. Feucht, F. Neukamm, A. Haufe, A phenomenological damage model to predict material failure in crashworthiness applications. Recent developments and innovative applications in computational mechanics: Springer, 2011, pp 143–153. https://doi.org/10.1007/978-3-642-17484-1_17

[13] V. Psyk, C. Scheffler, M. Tulke, S. Winter, C. Guilleaume, A. Brosius, Determination of Material and Failure Characteristics for High-Speed Forming via High-Speed Testing and Inverse Numerical Simulation, J. Manuf. Mater. Process. 4 (2020), Nr. 2, pp. 31. https://doi.org/10.3390/jmmp4020031

[14] G.I. Taylor, H. Quinney, The latent energy remaining in a metal after cold working. In: Proceedings of the Royal Society of London. Series A, Containing Papers of a Mathematical and Physical Character 143 (1934), Nr. 849, pp. 307–326. https://doi.org/10.1098/rspa.1934.0004

[15] C.K.C. Lieou, C.A. Bronkhorst, Thermomechanical conversion in metals: dislocation plasticity model evaluation of the Taylor-Quinney coefficient, Acta Mater. 202 (2021), Nr. 849, pp. 170–180. https://doi.org/10.1016/j.actamat.2020.10.037